Pramāṇa, Vol. 19, No. 3, September 1982, pp. 203–213. © Printed in India.

Temperature variation of the Debye-Waller factors of Ba^{++} and F^- ions in BaF_2 powder by x-ray diffraction

R SRINIVASAN and K S GIRIRAJAN*
Department of Physics, Indian Institute of Technology, Madras 600,036 India
*Department of Crystallography and Biophysics, University of Madras, Guindy Campus, Madras 600 025, India

MS received 1 April 1982; revised 10 July 1982

Abstract. The temperature variation of the Debye-Waller factors of Ba^{++} and F^- ions in BaF_2 powder has been studied using x-ray powder diffraction over the temperature range 77°–298°K. A continuous flow cryostat has been specially fabricated for this purpose for the YPC 50 NM powder diffractometer available in the department. The Debye-Waller factors of Ba^{++} and F^- between room temperature and 879°K have been measured using single crystal neutron diffraction by Cooper *et al*. Theoretical lattice dynamics shell model calculations using a 7-parameter model in a quasi-harmonic approximation have been done over a temperature range 77° to 879°K. The theoretical values have been compared with the present x-ray measurements and the single crystal neutron diffraction values and the results are discussed.

Keywords. Cryostat; powder diffraction; Debye-Waller factor; lattice dynamics; barium fluoride.

1. Introduction

The lattice dynamics of the fluorides of calcium, strontium and barium has been studied theoretically and experimentally. The phonon dispersion relations in calcium and strontium fluorides have been experimentally studied by inelastic neutron scattering and the parameters for a shell model fit of the dispersion relations are given by Elcombe and Pryor (1970) and Elcombe (1972). The Debye-Waller factors of the metal and fluorine atoms in these two crystals have also been measured by both x-rays (Togawa 1964; Strock and Batterman 1972; Mair and Barnea 1971 and Cooper 1970) and neutron diffraction (Cheetham *et al* 1971, Cooper and Rouse 1971) at room temperature and found to agree with the values calculated in a shell model in the harmonic approximation. The dispersion relations in barium fluoride were also determined by inelastic neutron scattering by Hurrell and Minkiewicz (1970). Using neutron diffraction Thomas (1976) has independently measured the temperature variation of the mean square displacements of Ba^{++} and F^- in BaF_2 powder from 673 to 1423°K. However, there is no attempt in his work to correct for Thermal diffuse scattering (TDS). Cooper *et al* (1968) have measured the Debye-Waller factors of Ba^{++} and F^- using neutron diffraction from 293 to 879°K. The theoretical values calculated on the harmonic approximation were in reasonable agreement with experiment at room temperature. But at high temperatures the experimental values of the Debye-Waller factors were larger than the theoretical values. This discrepancy

was attributed to anharmonicity. There are no experimental measurements on the temperature dependence of the Debye-Waller factors below room temperature.

In this paper we describe a cryostatic attachment to an existing powder diffractometer YPC 50 NM and report on the measurements on a powder sample of BaF_2. Section 2 describes the cryostatic attachment and other details of measurement. Section 3 deals with analysis of experimental data and presents the results on the temperature variation of the Debye-Waller factors of barium and fluorine. Section 4 gives the details of a theoretical calculation on a shell model and a comparison between theory and experiment.

2. Experimental details

2.1 *Continuous flow cryostat*

To cool the specimen and maintain it at any temperature below 300°K, a cryostatic attachment using the continuous flow principle was designed and fabricated to fit the Russian YPC-50 NM powder diffractometer. A schematic diagram of the cryostat is shown in figure 1.

The cryostatic attachment consists of three parts: (a) the cooling system, (b) the vacuum chamber and (c) a transparent window for visual inspection. The parts (a) and (b) are demountable.

(a) The cooling system consists of a square copper block (60 × 60 mm) on one face of which a cylindrical groove of 35 mm diameter and 2mm depth is cut. The powder specimen fits compactly in this groove. The copper plate is positioned in such a way that the x-ray beam from a line source falls on the powder sample only and not on any part on the copper mount. Four horizontal holes drilled parallel to the surface of the copper plate are interconnected to form a channel for the flow of liquid nitrogen. Liquid nitrogen flows from a small double-walled stainless steel vessel (capacity 200 ml) down a stainless steel tube which is brazed to the inlet of the channel in the copper plate. The stainless steel tube is surrounded by a larger stainless steel tube which is brazed to the former at its top end. The interspace between the tubes as well as the

Figure 1. Schematic diagram of the cryostat. (1) Vacuum gauge (2) leads of the electromagnet (3) neoprene 'O' ring (4) temperature regulator (5) flexible stainless steel bellow (6) sensor for indicating liquid nitrogen level (7) coil for the electromagnet (8) liquid nitrogen inlet from the main storage dewar (9) soft iorn core of the electromagnet (10) soft iron diaphragm (11) double-walled s.s. dewar of the cryostat (12) styroform lining (13) leads of the Cu-constantan thermocouple (14) leads of the heater elements if any or can be blinded (15) outer stainless steel tube of the s.s. dewar (16) suction end of the cryostat (17) brass flange which houses the cryostat (18) neoprene '0' ring (19) liquid nitrogen inlet tube of the cryostat (20) liquid nitrogen outlet tube of the cryostat (21) aluminium ring of the vacuum chamber (22) channel for flow of liquid nitrogen (23) transparent perspex ring allows provision for visual inspection (24) copper plate on which the sample is cooled (25) Mylar window (26) circular groove in which the sample is kept (27) adjustable mount for the cryostat assembly (28) bolts for fixing the cryostat on the adjustable mount (29) dovetail type of arrangement which allows lateral back and front movement of the cryostat (30) the brass plates which house the screw and spring to provide the lateral movement (31) graduated disc in which the translatory portion of the mount sits (32) brass plates housing the spring and screw to provide the rotation adjustment (33) bolts which fix the adjustable mount and the cryostat on the central spindle of the diffractometer (34) screws which provide the lateral back and forth movement of the cryostat (35) central spindle of the diffractometer.

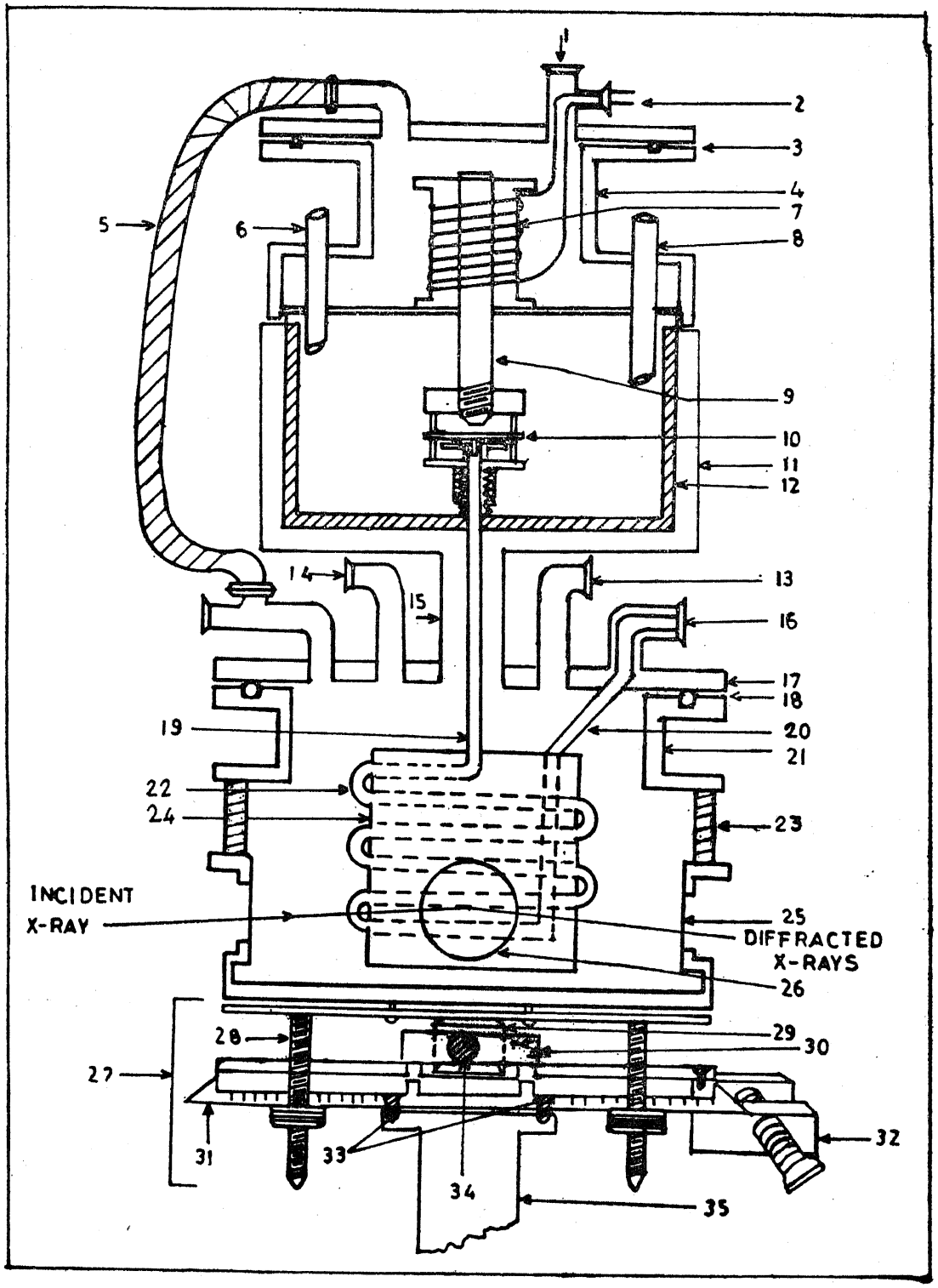
1
2
3
4
5
6
7
8
9
10
11
12
13
14
15
16
17
18
19
20
21
22
24
23
INCIDENT
X-RAY
25
DIFFRACTED
X-RAYS
26
27
28
29
30
31
33
34
35
32

Figure 1.

interspace between the walls of the dewar gets pumped down as the vacuum chamber is evacuated. The nitrogen gas emerging from the copper plate flows through another thin walled stainless steel tube ending in a NW 10 connection. By connecting a rotary vacuum pump to the NW 10 flange a steady stream of nitrogen flows through the copper block. The rate of nitrogen flow can be controlled by having a needle valve between the pump and the NW 10 flange. The outer wall of the stainless steel dewar and the outer tube of the NW 10 flange are firmly brazed to a circular brass flange. There are other outlets on the brass flange to take the electrical leads out.

(b) The vacuum chamber in which the specimen is kept consists of a cylindrical aluminium vessel with a top flange equal in diameter to the brass flange of the cryostat. Three symmetric windows (spanning an angle of 120° each at the centre) are cut around the circumference. These are covered with a mylar sheet, 10 mil thick to enable the inside of the vessel to be evacuated. At the same time these mylar windows serve for the entrance and exit of x-rays. The chamber is evacuated with a diffusion pump after assembly to a vacuum better than 10^{-4} torr.

(c) The transparent window is made of a perspex ring which is fastened at its bottom with the top flange of the portion of the vacuum chamber consisting of the mylar window and at its top with a flange on an aluminium ring. The top flange of the aluminium ring mates with the brass flange of the continuous flow cryostat. The transparent perspex window allows a visual inspection of the sample and the thermocouple leads after the entire system is mounted in the diffractometer. Neoprene 'O' rings provide the vacuum seal between the mating flanges.

2.2 *Adjustable mount for centering the specimen on the diffractometer*

After assembling, the cooling system is mounted so that the entire system is rotated about the central axis. In order to align the sample so that it lies exactly on the axis of rotation, an adjustable mount was specially designed. Using this mount it is possible to translate the cryostat by about $\pm$ 5 mm and to rotate the cryostat through an angle of 5° either way about the vertical. Using these adjustments it is possible to obtain a perfect alignment of the sample.

2.3 *Temperature measurement and control*

The temperature is measured by a standard copper-constantan thermocouple. Temperature regulation is obtained by regulating the flow of liquid nitrogen through the cryostat. The tube through which liquid nitrogen flows down from the dewar to the cryostat is provided with a flange fitted with a teflon 'O' ring. A soft iron diaphragm actuated by an electromagnet closes the flange and prevents the flow of liquid nitrogen. The e.m.f. of the thermocouple is compared with a preset value on the temperature controller. When the specimen temperature is less than the value required the electromagnetic valve opens allowing the flow of liquid nitrogen. On the other hand, when the specimen is colder than the required value the valve closes preventing the flow of nitrogen. With such an arrangement it was possible to keep the specimen temperature constant to within $\pm$ 0·1° for long periods in the range

300 to 77°K. A needle valve kept at the mouth of the rotary pump connected to the cryostat also helps in reaching different temperatures quickly. In order to keep a steady flow of liquid nitrogen the level of the liquid nitrogen in the stainless steel dewar is maintained constant by an automatic transfer from a larger storage dewar.

2.4 *Details of measurement*

Supra pure BaF_2 supplied by Merck was ground to a fine powder which will pass through a 325 mesh screen. After applying a little vacuum grease in the slot of the copper plate to improve thermal contact, the powdered barium fluoride was filled into the slot and pressed to have a smooth surface.

The cryostat was then assembled and mounted on the centre spindle of the diffractometer. The sample was properly centred using the adjustable mount. The vacuum chamber was evacuated to a vacuum better than 10^{-4} torr before the experiment was started. Copper K_α radiation was used with nickel filter. The diffractograms of the various reflections were recorded using a speed of rotation of the specimen of 1/4° per minute. At each temperature the diffractograms were recorded at least two to three times to check reproducibility. The diffractograms were recorded at six different temperatures between room temperature and liquid nitrogen.

To check if the sample temperature was truly that recorded by the thermocouple the mean thermal expansion coefficient of BaF_2 between room temperature and the temperature of measurement was calculated from the shift in the prominent higher angle Bragg peaks. The values so calculated were found to be in agreement with the values reported by Bailey and Yates 1967 to within 5%.

3. Analysis of experimental data

The procedure adopted by Togawa (1964) for CaF_2 is followed in analysing the present results. Except for the (111) reflection the diffractograms for other reflections showed two distinct but close peaks due to λ_1 and λ_2. In order to estimate the background the diffractograms were recorded over a range of $\pm 2°$ around the double peaks and the background was estimated by a smooth interpolation between the two extreme ends of the diffractograms. The area under the double peak was measured after correcting for the background. The weighted mean value λ of the wavelength is used in further calculations.

In BaF_2 one can distinguish between three types of reflections.

(a) reflections for which $(h + k + l)$ is an odd integer. The structure factor F for these reflections is given by

$$F = 4 f(Ba^{++}), \tag{1}$$

where $f(Ba^{++})$ is the atomic scattering factor of doubly-ionised barium.

(b) reflections for which $h + k + l = 4n$ where n is an integer. The structure factor,

$$F = 4\,[f(Ba^{++}) + 2 f(F^-)]. \tag{2}$$

(c) reflections for which $h + k + l = 4n + 2$ where n is zero or an integer. The structure factor is

$$F = 4\,[f(Ba^{++}) - 2 f(F^-)]. \tag{3}$$

In evaluating the atomic scattering factor one uses an analytical expression

$$f = \sum_{i=1}^{4} a_i \exp - b_i \sin \theta/\lambda + c; \tag{4}$$

the constants a_i, b_i and c for Ba^{++} and F^- being taken from the International Tables for X-ray Crystallography (1974). In evaluating F, the dispersion correction for Ba is taken into account in the usual way.

The integrated area under the peak is related to the structure factors by the following relations for the three cases.

(i) $$A^a = K_a\,(mLp)\,[f(Ba^{++}) \exp - B\,(Ba^{++}) \sin^2 \theta/\lambda^2]^2,$$

(ii) $$A^b = K_b\,(mLp)\,[f(Ba^{++}) \exp - B\,(Ba^{++}) \sin^2 \theta/\lambda^2 + 2f(F^-) \exp - B\,(F^-) \sin^2 \theta/\lambda^2]^2,$$

(iii) $$A^c = K_c\,(mLp)\,[f(Ba^{++}) \exp - B\,(Ba^{++}) \sin^2 \theta/\lambda^2 - 2f(F^-) \exp - B\,(F^-) \sin^2 \theta/\lambda^2]^2.$$

The factor 4^2 which arises from (1) to (3) is absorbed in the constants K_a, K_b and K_c. In the above m is the vector multiplicity, L_p the Lorentz polarisation factor, $B\,(Ba^{++})$ and $B\,(F^-)$ are the temperature factors for Ba^{++} and F^- respectively.

The odd reflections directly yield the values of $B(Ba^{++})$. A plot of

$$\ln \left\{ \frac{(A^a/mLp)^{1/2}}{f(Ba^{++})} \right\}$$

against $-\sin^2 \theta/\lambda^2$ can be fitted to a straight line whose slope yields $B\,(Ba^{++})$ and whose intercept on the y axis gives $\ln K_a^{1/2}$. Such plots for the reflections (111), (311), (331), (511), (333) and (531) at 298 and 78·2° K are shown in figures 2a and 2b respectively.

To arrive at $B(F^-)$ the intensities of reflections of type (b) are used. One must first estimate the value of K_b. As suggested by Togawa (1964) this is done by plotting,

$$\ln \left\{ \frac{(A^b/mLp)^{1/2}}{(f(Ba^{++}) + 2f(F^-))} \right\},$$

against $-\sin^2 \theta/\lambda^2$. In effect in finding an approximate value of K_b one assumes the same B factor for Ba^{++} and F^-. The intercept of the best fit straight line on the Y axis gives $\ln K_b^{1/2}$. Now from $(A^b/mLp)^{1/2}$ one substracts $K_b^{1/2}(f(Ba^{++}) \exp - B(Ba^{++}) \sin^2\theta/\lambda^2)$ using the value of $B(Ba^{++})$ obtained from an analysis of odd reflections, to get $(A^{b'}/mLp)^{1/2}$. A plot of

$$\ln \left\{ \frac{(A^{b'}/mLp)^{1/2}}{2f(F^-)} \right\}$$

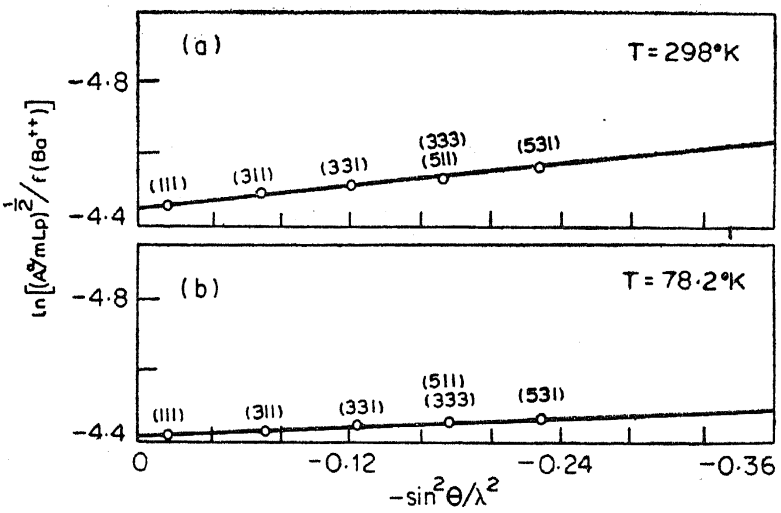

Figure 2. A plot of ln $[(A^a/mLp)^{1/2}/f(Ba^{++})]$ vs $-\sin^2\theta/\lambda^2$ for odd reflections at **a.** T = 298°K. **b.** T = 78·2°K.

against $-\sin^2\theta/\lambda^2$ yields a straight line whose slopes gives $B(F^-)$. Such plots are shown in figures 3a and 3b for the reflections (220), (400), (422), (440) and (620) at 298 and 78·2° K respectively.

The B factors deduced above ignored the correction due to thermal diffuse scattering. However from the B values so determined one may obtain the approximate correction for the first order thermal diffuse scattering using Chipman and Paskin's (1959) correction. After applying this correction to the measured intensities the analysis can be redone to give refined values of the B factors. Table 1 lists the experimental B factors for Ba^{++} and F^- at different temperatures with and without TDS correction. The atomic scattering factors of Ba^{++} and F^- for x-rays is approximately in the ratio 5:1. So one may have doubts about the reliability of using Togawa's procedure. The intensity data used in obtaining $B(Ba^{++})$ and $B(F^-)$ using Togawa's method were also directly refined on the IBM 370 computer using the iteration program written by Gantzel *et al* (1961) without applying TDS correction. This was done at 298 and 78·2°K. The values of $B(Ba^{++})$ and $B(F^-)$ obtained from the above program at 298°K are 0·55Å^2 and 0·97Å^2 with a final R factor of 0·4%, and at 78·2°K, 0·16Å^2, 0·37Å^2, with a final R factor of 0·1% respectively. These may be compared with the values of 0·57Å^2 and 0·93Å^2 at 298°K (without TDS) and 0·16Å^2 and 0·43Å^2 at 78·2°K using Togawa's method. If we compare the B factors obtained by different workers using the iteration method on a crystal such as CaF_2 one finds a variation of about 10% in the B values. The difference between the values obtained by Togawa's method and the iteration method in the present case is nearly within this limit.

The temperature factors for Ba^{++} and F^- were determined by Cooper *et al* (1968) above room temperature using neutron diffraction. In figure 4 are plotted the experimental values of $B(Ba^{++})$ and $B(F^-)$ determined below room temperature in the present experiment and the values determined by Cooper *et al* (1968) above room

Table 1. Experimental and theoretical values of B factors for Ba^{++} and F^- as a function of temperature

		Experimental values				Theoretical values			
No.	T°(K)	Without TDS $B(Ba^{++})$ (Å²)	With TDS $B(Ba^{++})$ (Å²)	Without TDS $B(F^-)$ (Å²)	With TDS $B(F^-)$ (Å²)	(har) $B(Ba^{++})$ (Å²)	(Q.har) $B(Ba^{++})$ (Å²)	(har) $B(F^-)$ (Å²)	(Q.har) $B(F^-)$ (Å²)
1.	78·2	0·16	0·17	0·43	0·44	0·17	0·17	0·40	0·40
2.	101·0	0·20	0·21	0·46	0·47	0·21	0·21	0·44	0·44
3.	125·8	0·22	$0·23_5$	0·47	0·48	0·25	0·25	0·49	0·49
4.	166·1	$0·28_6$	0·30	0·59	0·60	0·32	0·32	0·58	0·59
5.	200·2	$0·36_6$	0·38	0·68	0·69	0·38	0·38	0·67	0·68
6.	230·8	0·45	0·47	0·79	0·80	0·43	0·44	0·75	0·76
7.	258·7	$0·51_5$	0·54	0·89	$0·89_6$	0·48	0·49	0·83	0·84
8.	298·0	0·57	0·60	0·93	0·94	0·55	0·56	0·93	0·96
9.	293·0		0·68[a]		1·05	0·55	0·55	0·94	0·94
10.	361·0		0·79[a]		1·24	0·67	0·68	1·11	1·17
11.	432·0		0·98[a]		1·54	0·80	0·82	1·33	1·39
12.	512·0		1·24[a]		1·92	0·94	0·98	1·54	1·69
13.	590·0		1·44[a]		2·26	1·09	1·15	1·77	2·00
14.	671·0		1·72[a]		2·68	1·23	1·34	2·00	2·38
15.	879·0		2·26[a]		3·68	1·62	1·98	2·61	3·77

[a]Values of single crystal neutron diffraction from Cooper *et al.* (1968).

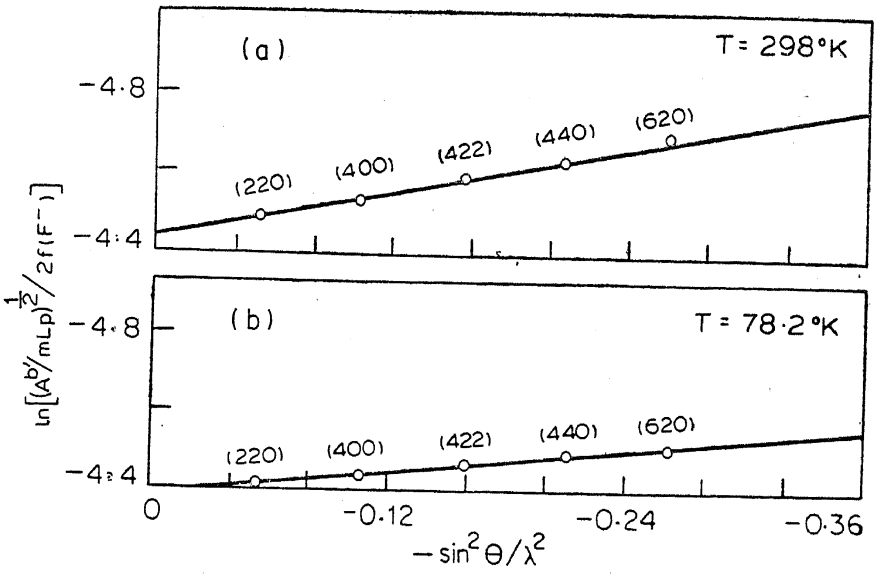

Figure 3. A plot of ln $[(A^b/mLp)^{1/2}/2f(F^-)]$ vs $-\sin^2\theta/\lambda^2$ for even reflections at **a.** T = 298°K. **b.** T = 78·2°K.

temperature. At room temperature the present values are in reasonable agreement with their measurements.

4. Theoretical calculations of the B factors in BaF_2 using the shell model

The dispersion relations in BaF_2 were determined by Hurrel and Minkiewicz (1970) who fitted a 11-parameter shell model to the experimental data. In calculating the equation of state of alkaline earth fluorides, Srinivasan and Ramachandran (1976) used a seven-parameter shell model which gave as good a fit to the dispersion curves as the 11-parameter model of Hurrel and Minkiewicz. This model has been used to compute the normal mode frequencies $\nu\begin{pmatrix}q\\j\end{pmatrix}$ and the eigen vectors $e\left(\mu\middle|\begin{matrix}\mathbf{q}\\j\end{matrix}\right)$, ($\mu = Ba^{++}$ or F^-) in the harmonic approximation. The B factor for ion μ is given by

$$B(\mu) = \frac{2\pi}{3}\frac{\hbar}{Nm(\mu)}\sum_{q,\,j,\,a}\frac{\left|e_a\left(\mu\middle|\begin{matrix}\mathbf{q}\\j\end{matrix}\right)\right|^2}{\nu\begin{pmatrix}\mathbf{q}\\j\end{pmatrix}}\left[2n\begin{pmatrix}\mathbf{q}\\j\end{pmatrix}+1\right] \tag{6}$$

Here N is the number of equally distributed wave vectors $\mathbf{q}$ in the Brillouin zone for which calculations are made, $m(\mu)$ mass of ion μ, j is the branch index, a the component index and

$$n\begin{pmatrix}\mathbf{q}\\j\end{pmatrix} = \left[\exp\left(\frac{h\nu\begin{pmatrix}\mathbf{q}\\j\end{pmatrix}}{k_B T}\right) - 1\right]^{-1} \tag{7}$$

where h is the Planck's constant, k_B the Boltzmann's constant and T the absolute temperature in degrees K.

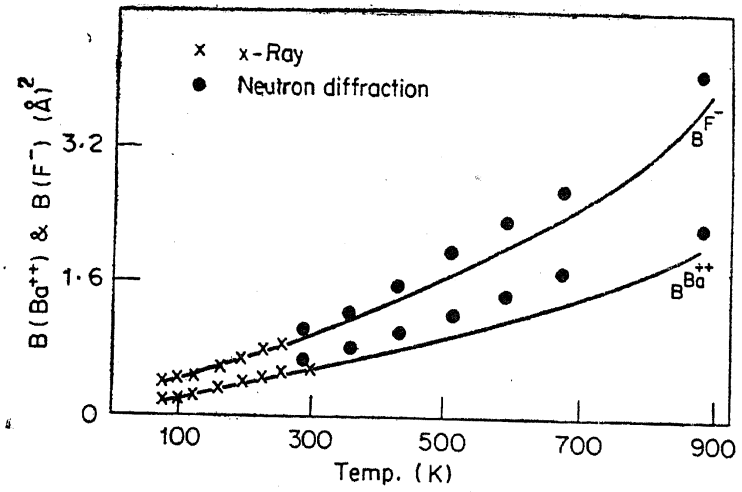

Figure 4. Temperature variation of the B factors for Ba^{++} and F^- ions in BaF_2 powder—x-rays, neutron diffraction and theory.

Two sets of calculations were performed, one in the harmonic approximation in which the frequencies of the lattice modes are assumed to be independent of temperature; and the other in the quasi-harmonic approximation where the normal mode frequencies vary with temperature due to lattice expansion. In the latter case the Grüneisen parameters of the modes were computed from the anharmonic parameters given by Srinivasan and Ramachandran (1976).

The calculations were carried out for 151 wave vectors in the irreducible part of the Brillouin zone on the IBM 1130 computer. The calculated B factors are given in table 1. The theoretical temperature variation of the B factors in the quasi harmonic approximation is depicted as continuous curves in figure 4 over the range 78·2 to 870°K. It is observed that the present measurements for Ba^{++} and F^- are in good agreement with theory. But above room temperature the neutron diffraction measurements of Cooper *et al* lie consistently above the theoretical curve.

It is noted that the results of Cooper *et al* at high temperatures are not in agreement even with the quasi-harmonic calculations which takes the effect of anharmonicity into account partially through the temperature dependence of the lattice frequencies. The full effects of anharmonicity will have to be involved to account for the deviations.

In conclusion the B factors for Ba^{++} or F^- have been measured over the range 78·2 to 293°K in BaF_2 and the experimental results are found to be in good agreement with the harmonic lattice dynamical calculations based on a 7-parameter shell model.

Acknowledgements

The encouragement and financial support granted by the Head of the Department of Crystallography & Biophysics of the University is gratefully acknowledged. The assistance given by the workshop staff of the above department, and the low temperature laboratory staff of IIT, Madras, is acknowledged with profuse gratitude. The program given by Dr V Ramachandran to calculate the lattice dynamics of fluorite lattice and the help rendered by Mr. Sivasubramanian of IBM 1130 Computer Centre to fit it in IBM 1130 computer is also gratefully acknowledged.

List of symbols

F	structure factor for x-ray scattering
$f(\mu)$	atomic scattering factor for ion μ
$B(\mu)$	temperature factor for ion μ
θ	Bragg angle of diffraction
λ	wavelength of x-ray used
Lp	Lorentz polarisation factor
m	vector multiplicity of a reflection
$A^aA^bA^c$	integrated area under a Bragg reflection peak corresponding to reflections of type a, b or c
$K_aK_bK_c$	scale factors
$\hbar$	Planck's constant divided by 2π
N	number of wave vectors in the Brillouin zone
$m(\mu)$	mass of ion of type μ
$\boldsymbol{q}$	wave vector of the lattice mode
j	branch index of the lattice mode
$\nu\begin{pmatrix}\boldsymbol{q}\\ \boldsymbol{j}\end{pmatrix}$	frequency of the normal mode belonging to the j branch at wave vector $\boldsymbol{q}$
k_B	Boltzmann's constant
T	absolute temperature

References

Bailey A C and Yates B 1967 *Proc. Phys. Soc. (London)* **91** 390
Cheetham A K, Fender B E F and Cooper M J 1971 *J. Phys.* **C4** 3107
Chipman D R and Paskin A J 1959 *J. Appl. Phys.* **30** 1998
Cooper M J 1970 *Acta Crystallogr.* **A26** 208
Cooper M J and Rouse K D 1971 *Acta Crystallogr.* **A27** 622
Cooper M J, Rouse K D and Willis B J M 1968 *Acta Crystallogr.* **A24** 484
Elcombe M M 1972 *J. Phys.* **C5** 2707
Elcombe M M and Pryor A W 1970 *J. Phys.* **C3** 492
Gantzel P K, Sparks R A and Trueblood K N 1961 University of California Program UCLALS 1
Hurrell J P and Minkiewicz V J 1970 *Solid State Commun.* **8** 463
International Tables for X-ray Crystallography 1974 (Birmingham, Kynoch Press), Vol. 4, p. 71, (Tables 2.2B)
Mair S L and Barnea Z 1971 *Phys. Lett* **A35** 286
Srinivasan R and Ramachandran V 1976 *Pramana* **6** 87
Strock H B and Batterman B W 1972 *Phys. Rev.* **B5** 2337
Thomas M W 1976 *Chem. Phys. Lett.* **40** 111
Togawa S 1964 *J. Phys. Soc. (Jpn.)* **19** 1696